



1 **Climate signals in a multispecies tree-ring network from central and**  
2 **southern Italy and reconstruction of the late summer temperatures**  
3 **since the early 1700s**

4  
5 Giovanni Leonelli<sup>1</sup>, Anna Coppola<sup>2</sup>, Maria Cristina Salvatore<sup>2</sup>, Carlo Baroni<sup>2,3</sup>, Giovanna Battipaglia<sup>4,5</sup>,  
6 Tiziana Gentilesca<sup>6</sup>, Francesco Ripullone<sup>6</sup>, Marco Borghetti<sup>6</sup>, Emanuele Conte<sup>7</sup>, Roberto Tognetti<sup>7</sup>, Marco  
7 Marchetti<sup>7</sup>, Fabio Lombardi<sup>8</sup>, Michele Brunetti<sup>9</sup>, Maurizio Maugeri<sup>9,10</sup>, Manuela Pelfini<sup>11</sup>, Paolo  
8 Cherubini<sup>12</sup>, Antonello Provenzale<sup>3</sup>, Valter Maggi<sup>1,3</sup>

9  
10 <sup>1</sup> Università degli Studi di Milano–Bicocca — Dept. of Earth and Environmental Science

11 <sup>2</sup> Università degli Studi di Pisa — Dept. of Earth Science

12 <sup>3</sup> Istituto di Geoscienze e Georisorse, Consiglio Nazionale delle Ricerche, Pisa

13 <sup>4</sup> Università della Campania — Dept. DiSTABIF

14 <sup>5</sup> University of Montpellier 2 (France) — PALECO EPHE

15 <sup>6</sup> Università degli Studi della Basilicata — School of Agricultural, Forestry, Food and Environmental Sciences, Potenza

16 <sup>7</sup> Università degli Studi del Molise — Dept. of Bioscience and Territory

17 <sup>8</sup> Università Mediterranea di Reggio Calabria — Dept. of Agronomy

18 <sup>9</sup> Istituto di Scienze dell'Atmosfera e del Clima, Consiglio Nazionale delle Ricerche, Bologna

19 <sup>10</sup> Università degli Studi di Milano — Dept. of Physics

20 <sup>11</sup> Università degli Studi di Milano — Dept. of Earth Science

21 <sup>12</sup> Swiss Federal Institute for Forest, Snow and Landscape Research WSL (Switzerland)

22 *Correspondence to:* Giovanni Leonelli ([giovanni.leonelli@unimib.it](mailto:giovanni.leonelli@unimib.it))

23 **Abstract.** A first assessment of the main climatic drivers that modulate the tree-ring width (RW) and maximum latewood  
24 density (MXD) along the Italian Peninsula and northeastern Sicily was performed using 27 forest sites, which include conifers  
25 (RW and MXD) and broadleaves (only RW). Tree-ring data were compared using the correlation analysis of the monthly and  
26 seasonal variables of temperature, precipitation and standardized precipitation index (SPI, used to characterize meteorological  
27 droughts) against each species-specific site chronology and against the highly sensitive to climate (HSTC) chronologies (based  
28 on selected indexed individual series). We find that climate signals in conifer MXD are stronger and more stable over time than  
29 those in conifer and broadleaf RW. In particular, conifer MXD variability is directly influenced by the late summer (August,  
30 September) temperature and is inversely influenced by the summer precipitation and droughts (SPI at a timescale of 3 months).  
31 Conifer RW is influenced by the temperature and drought of the previous summer, whereas broadleaf RW is more influenced by  
32 summer precipitation and drought of the current growing season. The reconstruction of the late summer temperatures for the  
33 Italian Peninsula for the past 300 yr, based on the HSTC chronology of conifer MXD, shows a stable model performance that  
34 underlines periods of climatic worsening around 1699, 1740, 1814, 1909, 1939 CE and well follows the variability of the  
35 instrumental record. Considering a 20 yr low-pass filtered series, the reconstructed temperature record consistently deviates  
36 <1°C from the instrumental record. This divergence may be due also to the precipitation patterns and drought stresses that  
37 influence the tree-ring MXD at our study sites. The reconstructed temperature variability is valid for the west-east oriented  
38 region including Sardinia, Sicily and the western Balkan area along the Adriatic coast.

39 **1 Introduction**

40 Reconstructions of climate for periods before instrumental records rely on proxy data from natural archives and on the ability to  
41 date them. The build-up of these 'natural archives' can exploit physical processes (e.g., ice cores, glacial landforms), biological  
42 growth processes (e.g., tree-rings, corals) or the direct interactions of these elements (e.g., pollen sequences in lacustrine  
43 deposits, or lake varves). The reading of sequences from these archives requires a deep understanding of the many complex



1 time-varying interactions between biotic and abiotic processes that characterize any ecosystem and may lead to relative or  
2 absolute chronologies with varying resolutions and time scales, which are different for each type of proxy. Among the various  
3 available proxies, tree rings are one of the most used datasets for reconstructing past climates with annual resolution in  
4 continental areas and are often from the temperature-limited environments with high latitudes and altitudes (e.g., Briffa et al.,  
5 2004; Rutherford et al., 2005). They can be used at the regional to global scales (IPCC, 2013) and long chronologies that can  
6 cover millennia, back as far as the early Holocene are available (for Europe: Becker, 1993; Friedrich et al., 2004; Nicolussi et al.,  
7 2009).

8 The reconstruction of past climate variability and the analysis of its effects on forest ecosystems is crucial for understanding  
9 climatic processes and for predicting what responses should be expected in ecosystems under the ongoing climatic and global  
10 changes. In particular, the Mediterranean region is a prominent climate change hot spot (Giorgi, 2006; Turco et al., 2015), and by  
11 the end of this century, it will likely experience a regional warming higher than the global mean (up to +5°C in summer) and a  
12 reduction of the average summer precipitation (up to -30 %; Somot et al., 2007; IPCC, 2013). The increase in droughts during  
13 the growing season is already negatively impacting tree growth, especially at xeric sites in the southwestern and eastern  
14 Mediterranean (e.g., Galván et al., 2014). At the ecosystem level, in the near future, the responses to climate changes will impact  
15 different forest species differently, depending on their physiological ability to acclimate and adapt to new environmental  
16 conditions (e.g., Battipaglia et al., 2009; Ripullone et al., 2009), and on their capacity to grow, accumulate biomass, and  
17 contribute as sinks in the terrestrial carbon cycle. Natural summer fires in the Mediterranean area are also expected to increase in  
18 frequency over the coming decades as a response to increasingly frequent drought conditions, assuming a lack of additional fire  
19 management and prevention measures (Turco et al., 2017). Furthermore, Mediterranean ecosystems are expected to experience  
20 the largest proportional change in biodiversity loss of any terrestrial ecosystem, since they are directly influenced by the major  
21 drivers of climate change and by land use-change (Sala et al., 2000).

## 22 1.1 Tree-ring Response to Climate

23 Climate-growth relationships have been studied for several species in the Mediterranean region, with different objectives: forest  
24 productivity (e.g., Biondi, 1999; Piovesan and Schirone, 2000; Boisvenue and Running, 2006; Nicault et al., 2008; Piovesan et  
25 al., 2008; Babst et al., 2013), forest trees ecophysiology, wood formation and related dating issues (Cherubini et al., 2003)  
26 sustainability of forest management (e.g., Boydak and Dogru, 1997; Barbati et al., 2007; Marchetti et al., 2010; Castagneri et al.,  
27 2014), provision of ecosystem services (e.g., Schröter et al., 2005) such as carbon sequestration (e.g., Scarascia-Mugnozza and  
28 Matteucci, 2014; Calfapietra et al., 2015; Borghetti et al., 2016 *in press*), effective biodiversity conservation (e.g., Todaro et al.,  
29 2007; Battipaglia et al., 2009), and climate reconstruction (see next heading), which has led to a variety of associations between  
30 climate variables and growth responses in conifers and broadleaves from different environments and ecosystems.

31 This study is focused on conifer and broadleaf forest sites located along the whole latitudinal range of the Italian Peninsula.  
32 Here, mainly considering the species of this study, we report the main findings on the climate-growth responses found in the  
33 Mediterranean region.

34 — *Conifers*. Studies on silver fir (*Abies alba* Mill.) growth in the Italian Peninsula reveal a distinct high sensitivity to the climate  
35 of the previous summer, August<sub>1</sub> in particular, positive correlations with precipitation and negative correlations with temperature  
36 (Carrer et al., 2010; Rita et al., 2014). Moreover, tree growth in this region is moderately negatively correlated to the temperature  
37 of the current summer (unlike that in stands located in the European Alps; Carrer et al., 2010), namely, high temperatures in July  
38 and August negatively affect tree growth. A dendroclimatic network of pines (*Pinus nigra* J.F. Arnold and *P. sylvestris* L.) in  
39 east-central Spain shows that drought (namely, the Standardized Precipitation-Evapotranspiration Index - SPEI; Vicente-Serrano  
40 et al., 2010) is the main climatic driver of tree-ring growth (Martin-Benito et al., 2013). Temperatures of the previous autumn  
41 (September) and of the current summer (July and August) have inverse effects on tree-ring growth, whereas growth is enhanced



1 by summer precipitation, especially in *P. sylvestris*; overall a higher influence from the climatic conditions of the previous year is  
2 seen in *P. nigra*. In a *P. uncinata* network from the Pyrenees, an increasing influence of summer droughts (SPEI) on tree-ring  
3 widths (RW) during the 20th century and the control of May temperatures on maximum latewood density (MXD) is found  
4 (Galván et al., 2015). However, in the proposed analyses, the possible influences of the summer climate variables from the year  
5 prior to the growth were not considered. Elevation, and particularly the related moisture regime, in the eastern Mediterranean  
6 region is the main driver of tree-ring growth patterns in a multispecies conifer network comprised of *P. nigra*, *P. sylvestris* and *P.*  
7 *pinea* L. specimens (Touchan et al., 2016). A dipole pattern in tree-ring growth variability is reported for Mediterranean pines  
8 ranging from Spain to Turkey (and Italy in the middle), with a higher sensitivity to summer drought in the east than in the west,  
9 and with a higher sensitivity to early summer temperature in the west (Seim et al., 2015). A strong correlation between autumn-  
10 to-summer precipitation and between summer drought and tree-ring growth is reported for sites (mainly of conifers) in northern  
11 Africa-western Mediterranean, with trees from Morocco also responding to the North Atlantic Oscillation Index (Touchan et al.,  
12 2017).

13 — *Broadleaves*. In the western Mediterranean (northern Morocco, Algeria, Tunisia, Italy and southern France), deciduous oaks,  
14 including *Quercus robur* L., reveal a direct response of tree-ring growth to summer precipitation and an inverse response to  
15 summer temperature (Tessier et al., 1994). Beech (*Fagus sylvatica* L.) is particularly sensitive to soil moisture and air humidity,  
16 and in past decades, long-term drought has been shown to be the main factor causing a growth decline in the old-growth stands  
17 in the Apennines (Piovesan et al., 2008). Moreover, beech shows different responses to climate at high- vs. low-altitude sites  
18 (Piovesan et al., 2005), with these latter, being positively affected by high May temperatures. Beech seems to present complex  
19 climate growth-responses and also appears to be a less responsive species in the Mediterranean area when compared to conifers  
20 such as *P. sylvestris*, *P. nigra*, *P. uncinata* or *A. alba* (as found in south-east France; Lebourgeois et al., 2012).

21 In all cases, the availability of long and reliable time series of meteorological variables, possibly from very close to forest sites,  
22 is crucial to estimating the climate-growth relationships. However, global or regional climatological datasets frequently lack  
23 local resolutions, especially in remote sites. We therefore decided to reconstruct climate variability more accurately, by  
24 considering local behaviors.

## 25 1.2 Tree-ring Based Climate Reconstructions

26 One of the most powerful tools in terrestrial paleoclimatology is obtaining dated information about the past climate and past  
27 environmental conditions in a region by analyzing the tree rings. However, in the Mediterranean region, the low temporal  
28 stability of the recorded climatic signals (e.g., Lebourgeois et al., 2012; Castagneri et al., 2014), the scarcity of long  
29 chronologies, and the high variability of climatic and ecological conditions (Cherubini et al., 2003) often make this analysis  
30 difficult. Ring widths are among the most used variables for climate reconstruction but usually show a higher temporal  
31 instability in their relationship with climate than that of maximum latewood density (for the Pyrenees, see Büntgen et al., 2010).

32 The potential to analyze relatively long chronologies in the Mediterranean region has allowed for the reconstruction of the past  
33 climate (precipitation and droughts, in particular) back to the 16th century. The 400-yr reconstruction of the October-May  
34 precipitation in Jordan allowed for the identification of dry conditions at the end of the 17th century and a higher variability in  
35 the recent decades 1960-1995 (using *Juniperus phoenicia* L. tree rings; Touchan et al., 1999). Reconstructed May-August  
36 precipitation for the eastern Mediterranean by means of a multi-species conifer network (mainly *P. sylvestris*, *P. nigra*, *Juniperus*  
37 *excelsa* M.Bieb. and *Cedrus libani* A.Rich.) has allowed researchers to identify the period of 1591-1595 as the longest sequence  
38 of consecutive dry years in the past 600 yr and the 1601–1605 and 1751–1755 periods as the wettest on record (Touchan et al.,  
39 2005a). Several reconstructions of May-June precipitation have been performed, mainly over the last 300-400 yr, in a region  
40 comprising northern Greece-Turkey-Georgia: in northern Aegean-northern Anatolia a tree-ring network of oaks was used for  
41 reconstructing precipitation variability since 1089 CE (Griggs et al., 2007); in the Anatolian Peninsula a mixed conifer-broadleaf



1 tree-ring network (mainly *P. nigra*, *P. sylvestris* and oaks; Akkemik et al., 2008), a *P. nigra* network (Köse et al., 2011) and a  
2 multi-species conifer network (mainly *P. nigra*, *P. sylvestris* and *Abies nordmanniana* (Steven) Spach; Köse et al., 2013) were  
3 used; in Caucasus a mixed conifer-broadleaf tree-ring network was used (mainly *P. sylvestris*, and *A. nordmanniana*;  
4 Martin-Benito et al., 2016). In the southern Anatolian Peninsula, April–August precipitation have been reconstructed using a *P.*  
5 *nigra* network (Akkemik and Aras, 2005) and in the northern Anatolian Peninsula besides the dominant signal of precipitation in  
6 these environments, March–April temperature have been reconstructed for the last 200 yr using a multispecies conifer network  
7 (Köse et al., 2017). In central Spain, a higher frequency of exceptionally dry summers has been detected since the beginning of  
8 the 20th century using a mixed tree-ring network of *Pinus sylvestris* and *P. nigra* ssp. *salzmannii* covering the past four centuries  
9 (Ruiz-Labourdette et al., 2014).

10 Reconstructions of past droughts and wet periods over the Mediterranean region have been created using climatic indices such as  
11 the Standardized Precipitation Index (SPI; McKee et al., 1995) in Spain (modeling 12-month July SPI using several species of  
12 the *Pinus* genre; Tejedor et al., 2016), in Turkey (modeling May–July SPI using *J. excelsa*; Touchan et al., 2005b) and in  
13 Romania (3-month August standardized SPI using *P. nigra*; Levanič et al., 2013), which allows for the identification of common  
14 large-scale synoptic patterns. Droughts have been reconstructed using the Palmer Drought Severity Index (PDSI; Palmer 1965).  
15 Using actual and estimated multispecies tree-ring data, Nicalut et al. (2008) found that the drought episodes at the end of the  
16 20th century are similar to those in the 16th–17th century for the western Mediterranean, whereas in the eastern parts of the  
17 region, the droughts seem to be the strongest recorded in the past 500 yrs.

18 The climate reconstruction of late summer temperatures published by Trouet (2014) for the period 1675–1980 CE in the  
19 northeastern Mediterranean-Balkan region, which used maximum latewood density chronologies, includes sites from the Italian  
20 Peninsula (used in this paper), the Balkan area, Greece and sites from the central and eastern European Alps to central Romania  
21 and Bulgaria, thus including areas characterized by continental climates. After carefully testing the climatic signals recorded in  
22 the tree-ring RW and MXD from different sites and different species, the reconstruction that is proposed in this study is the first  
23 one including only forest sites from the Italian Peninsula, which has a typical Mediterranean climatic regime at low altitudes and  
24 a Mediterranean-temperate regime at the higher altitudes of the Apennines.

25

26 Overall, the main objectives of this paper are:

- 27 (i) to identify the most important climatic drivers modulating tree-ring width (RW) and tree-ring maximum latewood density  
28 (MXD) variability in forest sites from central and southern Italy. To our knowledge, this is the first attempt performed in Italy  
29 with the clear objective to find common response patterns in conifer and broadleaf species using a multispecies tree-ring network  
30 and site-specific historical climatic records;
- 31 (ii) to estimate the temporal stability of the climate-growth and climate-density relationships;
- 32 (iii) to perform a climatic reconstruction based only on trees *highly sensitive to climate* (HSTC); and
- 33 (iv) to estimate the spatial coherence of the obtained reconstruction in the region.

## 34 2. Data and Methods

### 35 2.1 Study area and study sites

36 The study region includes the whole Italian Peninsula and eastern Sicily and covers a latitudinal range from 37° 46' N to 44° 43'  
37 N (Fig. 1). The peninsula is roughly oriented NW-SE and its longitudinal axis is characterized by the Apennines, a complex  
38 mountain chain caused by the Adria and African plates subducting under the Eurasian plate. The Apennines reach their  
39 maximum altitude at their center (Corno Grande Mt., 2912 m a.s.l., Gran Sasso Massif); a higher altitude is reached in eastern  
40 Sicily by the Etna Volcano (3350 m a.s.l.).



1 The study region is surrounded by the Tyrrhenian and Adriatic Seas and is characterized by a typical Mediterranean climate, with  
2 high temperatures and low precipitation during the summer (from June to September) (Fig. 2). Considering the climatic means at  
3 all of the study sites (at a mean elevation of  $1225\pm 520$  m a.s.l.) over the period of 1880-2014, the temperatures over the study  
4 region range from  $0.2^{\circ}\text{C}$  (January) to  $17.6^{\circ}\text{C}$  (in July and in August) and only 11 % of the total annual precipitation falls during  
5 the summer (from June to August: 155 mm), whereas 34 % falls during winter (from December<sub>1</sub> to February: 493 mm). Autumn  
6 is the second wettest season (31 % of total annual precipitation) and spring is the third wettest (24 % of total annual  
7 precipitation) (Fig. 2). For monthly temperatures, the standard deviations from the mean values at all sites are almost constant  
8 throughout the year ( $3.4^{\circ}\text{C}$ ), whereas precipitation ranges from 36.2 mm in July (corresponding to 88 % of the average July  
9 precipitation) to 129 mm in December (corresponding to 69 % of the average December precipitation).

10 The total forest cover in Italy, excluding the regions including the European Alps, is approximately 5.8 M hectares (Corpo  
11 Forestale dello Stato, 2005) which is 28 % of the surface. Forests characterize the landscape of the inner portion of the Apennine  
12 range, at mid to high elevations, and an additional 1.4 M hectares are covered by woodlands and shrublands, which are the so  
13 called Mediterranean ‘macchia’ that border the forests at low elevations and in areas relatively close to the sea. Overall,  
14 broadleaf species are much more abundant in the study region than conifer species, accounting for approximately  $\frac{3}{4}$  of the forest  
15 cover (Dafis, 1997).

16 The study sites are distributed along the whole latitudinal range of the Italian Peninsula and tree-ring proxies include both RW  
17 and MXD series collected within the NEXTDATA project, from Italian Universities, and from the ITRDB ([www.ncdc.noaa.gov](http://www.ncdc.noaa.gov);  
18 see Table 1 for full bibliographic references). The dataset is based on 27 forest sites composed of several species (conifers at 16  
19 sites, and broadleaves at 11 sites), from which tree-ring series of conifers (RW and MXD) and of broadleaves (RW) were  
20 prepared (Fig. 1, Table 1).

## 21 2.2 Climate variables

22 Synthetic records of monthly temperature and precipitation series were reconstructed to be representative of the sampled sites  
23 using the anomaly method (New et al., 2000; Mitchell and Jones, 2005), as described in Brunetti et al. (2012). The  
24 spatiotemporal structure of the signal of a meteorological variable over a given area can be described by the superposition of two  
25 fields: the climatological normals over a given reference period (i.e., the climatologies), which are characterized by distinct  
26 spatial gradients, and the departures from them (i.e., the anomalies), which are characterized by higher spatial coherence and  
27 linked to climate variability. Climatologies and anomalies were reconstructed independently of each other using different data  
28 sets (high spatial density and limited temporal coverage for the climatologies, and low spatial density but long temporal  
29 coverage and accurate homogenization for the anomalies). Climatologies were reconstructed following the procedure described  
30 in Brunetti et al. (2014) and Crespi et al. (2017), i.e., by estimating a local temperature (precipitation)-elevation relationship; the  
31 anomalies were reconstructed using weighted averages of high-quality and homogenized neighboring series from the improved  
32 dataset of Brunetti et al. (2006) (where the improvements consist of a new and more accurate homogenization of the early  
33 instrumental period) and records from the Italian Air Force network (Simolo et al., 2010). Finally, the two fields were  
34 superimposed to find the monthly temperature and precipitation series for each sampling site. The climate series start in different  
35 years due to data availability; however, most of the series start around the mid-19th century. Finally, in order to characterize  
36 meteorological drought conditions, the monthly Standardized Precipitation Index (SPI) was calculated at timescales of 1, 2, 3, 6,  
37 9 and 12 months for all of the sites, based on the monthly values of precipitation, using the SPI\_SL\_6 code of the National  
38 Drought Mitigation Center at the University of Nebraska (<http://drought.unl.edu>).

## 39 2.3 Chronology construction, climate sensitivity and climate reconstructions

40 — *Raw data*. All individual series of RW and MXD were examined for correct dating using visual and statistical crossdating. In



1 particular, statistical techniques were used to remove potential dating errors by comparing each individual series from one site  
2 against the mean site chronology, which was constructed without the analyzed individual series. Using the COFECHA software  
3 ([www.ldeo.columbia.edu](http://www.ldeo.columbia.edu)), the individual series are moved forward and backward 10 yr from their initial positions, and similarity  
4 indices are calculated over a 50-yr time window, thus highlighting the potential dating errors.

5 — *Site chronologies*. To preserve the low-frequency variability in the site chronologies, the Regional Curve Standardization  
6 approach (RCS; Briffa et al., 1992; Briffa and Melvin, 2011; Esper et al., 2003) was used both with the RW and MXD series. We  
7 used the ARSTAN software (ver. 44 h3, [www.ldeo.columbia.edu](http://www.ldeo.columbia.edu)) and did not consider the pith offset estimates between the first  
8 measured ring and the actual first year of growth. This approach does not significantly affect trends and temporal variability at  
9 any time scale in the resulting chronology (Esper et al., 2009; Leonelli et al., 2016). The regional curve (RC) for the mean  
10 chronology, which was obtained after the series alignment to the first measured ring, was smoothed using a cubic spline with a  
11 width of 10 % of the chronology length (Büntgen et al., 2006). Ratios of raw measurements vs. the values of growth predicted by  
12 the RC were computed for all years of the individual series, and the resulting indexed series were averaged by a biweight robust  
13 mean to obtain the site chronologies of RW and of MXD. The RW and MXD site chronologies were constructed only for sites  
14 with at least 10 individual series fulfilling the following conditions: i) the individual series length was >100 yr; ii) the individual  
15 series correlation with the respective site chronology had  $r > 0.3$ ; iii) the mean interseries correlation (MIC) had  $r > 0.3$ ; and iv)  
16 the expressed population signal (EPS; Wigley et al., 1984; Briffa and Jones, 1990) was > 0.7. Only the individual series fulfilling  
17 these conditions were used to construct the site chronologies. However, some exceptions were accepted in order to maximize the  
18 number of sites and chronologies available for analysis (see exceptions in Table 1).

19 — *Climate sensitivity*. Species-specific climate sensitivity was assessed for the constructed RW and MXD site chronologies over  
20 the common period of 1880-1980 using correlation analysis using the site-specific monthly variables of temperature,  
21 precipitation and Standardized Precipitation Index, from March of the year prior to growth to September of the year of growth.  
22 Correlations were computed using the DENDROCLIM software (Biondi and Waikul, 2004), applying a bootstrap with 1,000  
23 iterations, and the obtained results were analyzed by grouping together conifer and broadleaf species. The results of the climate  
24 sensitivity analysis were used to detect the *driving climate variables* (DCV; of temperature, precipitation and SPI) for each of the  
25 three groups of chronologies: MXD conifer, RW conifer and RW broadleaf. Specifically, for each group of chronologies and for  
26 each climate variable, the months with significant correlations at most sites (>50 %) and with mean correlation values of  $|\bar{r}| >$   
27 0.25 were identified (black-filled squares in Fig. 3). Then, from these months, six DCV were constructed by calculating z-scores  
28 and mean departures at each site and then completing the series; a final conversion to temperature and precipitation values was  
29 performed before the values were averaged between the sites, thus creating yearly records of the regionalized monthly climate  
30 variables; these records were then averaged between two to four consecutive months (according to what was obtained; see the  
31 black-filled squares in Fig. 3), finally obtaining the six DCV.

32 — *HSTC chronologies*. Based on the available RW and MXD indexed individual series from all of the sites, six HSTC  
33 chronologies were constructed, as in Leonelli et al. (2016). However, given the smaller number of datasets available in this study  
34 and the shortness of the time series, a modified version of the method was applied. In the present the method, all of the RW  
35 (conifer and broadleaf) and MXD (only conifer) indexed individual series were tested against each of the above-defined six  
36 DCV, and only the individual tree-ring indexed series with correlation values of  $|\bar{r}| > 0.25$  in both of the 100 yr subperiods of the  
37 climatic dataset (1781-1880 and 1881-1980) were used to build each of the six HSTC chronologies, which was done by simply  
38 averaging together the selected indexed series. The six HSTC chronologies were constructed starting from all of the indexed  
39 individual series of conifer MXD (148 series), of conifer RW (245) and of broadleaf RW (140), which were previously obtained  
40 while constructing the site chronologies (also, the indexed individual series from sites not meeting the fixed quality standards for  
41 a site chronology were included at the beginning of the selection).

42 — *Climate sensitivity through time*. To test the stability of the climate signals recorded in the HSTC chronologies, a moving



1 correlation analysis was conducted between the six HSTC chronologies and their respective DCV, computing bootstrapped  
2 correlation coefficients with DENDROCLIM over 60 yr time windows that were moved one year per iteration over the longest  
3 available periods.

4 — *Climate reconstruction.* The climate reconstruction used only the HSTC chronology showing the highest absolute values of  
5 correlation and the most stable signal over time (i.e., the conifer MXD for late summer temperature; see Results). To extend this  
6 HSTC chronology as far back in time as possible, the oldest available individual MXD indexed series with correlations of  $|\bar{r}| >$   
7 0.25 with this chronology and that had a minimum length of 100 yr were added. Linear regression and scaling models (Esper et  
8 al., 2005) were calibrated and verified over the periods of 1781–1880 and 1881–1980, respectively, and then the same was done  
9 over the inverted periods, in order to estimate model performances and stability. Reduction of error (RE; Fritts, 1976) and  
10 coefficient of efficiency (CE; Briffa et al., 1988) statistics were computed to assess the quality of the reconstructions. The  
11 reconstructed series of late summer temperatures were then used over the period 1901–1980 to build a spatial correlation map  
12 with the KNMI Climate Explorer (<http://www.climexp.knmi.nl>; Trouet and Oldenborgh, 2013), using the 0.5° grid of August–  
13 September average temperature (CRU TS/E-OBS 13.1; 1901–2009; Mitchell and Jones, 2005; Haylock et al., 2008) and  
14 considering only the grid points with over 30 % valid values. This independent dataset was used instead of the Italian one, as the  
15 primary goal was to analyze how far from the Italian Peninsula the reconstructed climatology is still representative.

### 16 3 Results

17 — *Site chronologies.* Fifteen RW site chronologies (11 from conifers and 4 from broadleaves) and eight MXD site chronologies  
18 (from conifers) were obtained and were used to estimate climate sensitivity at the site level and to detect the most important  
19 climatic drivers over the study region (for species percentages, see boxes in Fig. 3A, 3A' and 3A''). The construction of the  
20 HSTC chronologies (for the analysis of the temporal stability of climate signals and for climate reconstruction) was performed  
21 using also the individual series from the twelve sites (5 from conifer and 7 from broadleaves; see Table 1, gray-shaded areas in  
22 Table 2 and Methods) for which the site chronologies did not meet the quality standards. The maximum time span of tree-ring  
23 data covers the period from 1415 (ITRDBITAL015) to 2013 CE (QFIMP1 and QFIMP2). However, the mean chronology length  
24 is  $215 \pm 130$  yr for conifers and of  $175 \pm 25$  yr for broadleaves (values rounded to the nearest 5 yr; Table 2). Over the common  
25 period considered (1880–1980 for all MXD and RW chronologies) the mean series intercorrelation and expressed population  
26 signal are approximately 0.5 and 0.8, respectively.

27 — *Tree-ring sensitivity to climate.* The site-specific sensitivity analysis performed over the common period of 1880–1980 reveals  
28 that MXD in conifers records stronger climatic signals than RW in either conifers or broadleaves, in terms of the average  
29 correlation coefficient, the number of months showing statistically significant values ( $p < 0.05$ ) and the fraction of chronologies  
30 (over the maximum number available) responding to the same climatic variable (Fig. 3). In particular, all conifer MXD  
31 chronologies are positively influenced by late summer temperatures (August and September), whereas precipitation from June to  
32 August is negatively correlated with most of them (Fig. 3A and 3B). In terms of SPI, the highest correlations (for both MXD and  
33 RW) were obtained for the indices calculated at the timescales of 2 and mainly of 3 months (SPI\_3; only the latter is reported in  
34 the Results), while longer timescales showed fewer significant correlation values. Most conifer MXD are negatively correlated  
35 with SPI\_3 from June to September, highlighting that low index values, i.e., drought periods, are associated with high MXD in  
36 the tree rings, and vice versa (Fig. 3C).

37 For conifer RW, significant correlation coefficients, i.e., those exceeding the mean value of  $|\bar{r}| > 0.25$  for more than 50 % of the  
38 available chronologies, were obtained only for the August temperatures of the year prior to growth (a negative correlation; Fig.  
39 3A'). In the other months, correlations are generally low and sometimes show opposite signs for the same climatic variable.  
40 However, a slightly stronger influence from the climatic variables for the summer months prior to growth is noted (black areas in



1 Fig. 3A', 3B' and 3C').

2 Broadleaf RW are positively influenced by high precipitations and low drought occurrences (high SPI\_3 values) during the  
3 summer months (June and July precipitation and June to August SPI\_3; Fig. 3B'' and 3C''), whereas the temperature does not  
4 show a significant influence (Fig. 3A'').

5 — *Stability of the climatic signal over time.* The six comparisons performed between the HSTC chronologies and the DCV were  
6 deemed important to understand the influence of the climate over time on conifers MXD and RW and on broadleaf RW (Fig. 4).  
7 The moving-window correlation analysis reveals that the HSTC conifer MXD chronology holds the strongest and most stable  
8 climatic signal of late summer temperature over time, with values ranging from approximately 0.4 to nearly 0.8 in the more  
9 modern periods analyzed (#1 in Fig. 4). In the other two HSTC chronologies based on conifer MXD (#2 and #3 in Fig. 4),  
10 starting from the time window 1881-1940 up to recent periods, we always find higher absolute values for SPI\_3 than for  
11 precipitation, with values of correlation reaching approximately -0.7 and -0.6, respectively, (#3 and #2 in Fig. 4). For the conifer  
12 RW, a strong change in the temperature signal of August prior to growth is found (#4 in Fig. 4), with correlation values shifting  
13 from positive (and statistically non significant) in the early period of analysis to negative (approximately -0.5) in the mid to late  
14 period of analysis. The two HSTC chronologies of broadleaf RW show nearly the same correlation values and similar patterns  
15 with both the June and July precipitation and the June to August SPI\_3, with values at approximately +0.5 (#5 and #6 in Fig. 4).

16 — *Climate reconstruction.* The reconstruction of the late summer temperature for the Italian Peninsula was therefore based on  
17 the HSTC chronology of conifer MXD, while the conifer RW chronology was disregarded due to its low signal stability over  
18 time. The reconstructed series based on the scaling approach starts in 1657 and has a minimum sample replication of ten trees  
19 since 1713 CE (Fig. 5A); it well reproduces the variability of the instrumental record and underlines the periods of climatic  
20 worsening around 1699, 1740, 1814, 1909 and 1939 CE. The low-pass filtered series emphasize the mid-length fluctuations and  
21 show evidence of periods of temperature underestimations (centered around 1799, 1925 and 1952 CE) and of overestimations  
22 (around 1846) (Fig. 5B); however, the differences from the instrumental record are always within 1° C for both scaling and  
23 regression approaches. The two models show similar statistics for RE, which tends to have higher values when the models are  
24 calibrated for the period 1781-1880 and lower values when they are calibrated for the period 1881-1980 (Table 3). The CE  
25 statistics show similar patterns of RE, are always positive for the regression model, whereas for scaling, CE has a slightly  
26 negative value when the model is calibrated for the 1881-1980 period.

27 — *Spatial coherence of the reconstruction.* The spatial coherence of the late summer temperature reconstruction of the Italian  
28 Peninsula performed over the Mediterranean region shows that, for the period of 1901-1980 (defined by the beginning of the  
29 CRU TS/E-OBS 13.1 climate series and the end of the MXD series), the reconstructed series well predict the temperature  
30 variability in the west-east region around the Apennines (Fig. 6), whereas just a few kilometers north of the Apennines (in the Po  
31 Plane) and west the Balkan area (in Slovenia and Hungary), and eastwards, the correlation drops below 0.6. In detail, the  
32 reconstructed temperature highly correlates westward up to Sicily and Sardinia, and eastward to the western Balkan area along  
33 the Adriatic Sea up to northern Greece, whereas r values are already lower than 0.5 in a wide arch including northern Tunisia,  
34 southern France, the inner range of the European Alps, Turkey and southern Anatolia (Fig. 6).

#### 35 4 Discussion

36 The climate signals recorded in the multispecies and multiproxy tree-ring network from the Italian Peninsula reveal a general  
37 coherence with other climate-growth analyses performed in Mediterranean environments. As found in the Pyrenees for a conifer  
38 tree-ring network (Büntgen et al., 2010), we find generally strong and coherent signals between species when considering their  
39 MXD. In particular, in our record, the late summer temperature is well recorded in MXD chronologies, and the correlations with  
40 climate are stable over time. The MXD chronologies are mainly related to temperature; however, we found clear signals of the



1 influence of summer precipitation and droughts. In the Mediterranean area, especially during summer, high temperature is often  
2 associated with low precipitation and drought; therefore, when interpreting the temperature reconstructions based on tree-ring  
3 MXD in the Mediterranean area, also the associated influence of precipitation and droughts on MXD should be taken in account.  
4 The SPI, which is used here to represent drought conditions, was found to have higher correlations with both MXD and RW for  
5 the index calculated at the timescales of 2 and mainly of 3 months (whereas lower correlations are found at lower (1 month) and  
6 higher (6, 9 and 12 months) timescales); trees respond to the drought signal at this time timescale, which reflects soil moisture  
7 droughts in the root zone (the SPI\_3 is also the index used for modeling agricultural droughts, see e.g., WMO, 2012). On the  
8 other hand, trees do not respond to the signal of hydrological droughts at the catchment level (SPI at timescales of above 6  
9 months).

10 The reconstructed series of the late summer temperatures for the Italian Peninsula show a strong coherence with the instrumental  
11 record and with the reconstruction proposed by Trouet (2014) for the northeastern Mediterranean-Balkan region (Fig. 5C). The  
12 two reconstructions are highly consistent; the reconstruction of Trouet (2014) also includes the sites used in this paper. However,  
13 there are some differences between the two reconstructions: the reconstructed temperature in the Italian Peninsula tends to be  
14 generally less variable over time than in the Balkan area, and while periods of climatic worsening were recorded in both areas in  
15 1741 and 1814, similar events were seen in 1913 and in 1977 in the Balkan area alone. Interestingly, the periods of the larger  
16 differences between the reconstructed temperature and the instrumental records (around 1799, 1846, 1925 and 1952) are also  
17 those with stronger coherences between the two reconstructions, suggesting a regional coherence in the responses to climate,  
18 possibly facilitated by similar precipitation patterns in the two regions during the late summer.

19 The Apennines and the European Alps often show similar annual changes in precipitation. However, in some periods, they show  
20 opposite decadal trends, such as after 1830, when precipitation was increasing in the north of Italy but decreasing in the south,  
21 and after 2000, when the opposite behavior was observed (Brunetti et al., 2006). In the Italian Peninsula, the summer (JJA) and  
22 the autumn (SON) precipitation in 1835-1845 showed local minimum values in the instrumental record, likely inducing higher  
23 densities in the tree-ring latewood and therefore overestimations in model temperature values (Fig. 5B). Moreover, uncertainties  
24 between the instrumental records and MXD may rise given that trees do not respond linearly to high temperatures, resulting in  
25 divergences between climatological and MXD records (e.g., for the Alps and Europe, Battipaglia et al., 2010). As found in this  
26 study, MXD is influenced by both late-summer temperature and summer precipitation and drought. In the Mediterranean, these  
27 variables are usually negatively correlated. Therefore, in some periods, a given value of MXD could have been caused either by  
28 temperature and less by drought or vice versa.

29  
30 Climatic signals recorded in RW tree-ring chronologies of conifers and broadleaves show fewer clear common patterns in their  
31 correlations with climate variables than conifer MXD, although some climatic signals, which are valuable for climate  
32 reconstructions and for understanding climate impacts on tree-ring growth, were detected. In our records, the summer drought  
33 signal was clearly recorded at all broadleaf sites (Fig. 3C''), with moist periods (low recurrence of drought, i.e., high SPI\_3  
34 values) positively affecting tree-ring growth. This signal was fairly stable over time (Fig. 4), suggesting the possibility for  
35 climate drought reconstructions in the Italian Peninsula with the availability of longer dendrochronological series. The signal of  
36 previous August temperatures recorded in conifer chronologies (Fig. 3A') is too variable over time to allow for a reconstruction  
37 (Fig. 4). Here, the change in sensitivity is probably related to the negative effect of droughts in the summer and autumn (June to  
38 October) prior to growth (see SPI\_3 correlations; Fig. 3C'). The question of the temporal stability of climate-growth  
39 relationships is sometimes underestimated in climate reconstructions, even though changes of climate signals over time have  
40 been identified in the Mediterranean region (Lebourgeois et al., 2012; Castagneri et al., 2014) and in the European Alps (Leonelli  
41 et al., 2009; Coppola et al., 2012). Many environmental and physiological factors may influence tree growth processes and tree-  
42 ring sensitivities to climate, such as the still-debated fertilization effect due to increasing CO<sub>2</sub> concentration in the atmosphere



1 (e.g., Brienen et al., 2012). On the other hand, biomass production and tree growth in Mediterranean forests seem to be linked to  
2 nutrient availability and environmental constraints rather than to the availability of CO<sub>2</sub> (e.g., Jacoby and D'Arrigo, 1997;  
3 Körner, 2003; Palacio et al., 2013). Local low-energy geomorphological processes, such as sheetfloods (e.g., Pelfini et al., 2006),  
4 air/soil pollution linked to SO<sub>2</sub>, NO<sub>2</sub>, or O<sub>3</sub> depositions and dust depositions from industrial plants or mines (in central Europe;  
5 Elling et al., 2009, Kern et al., 2009; Sensula et al., 2015), may influence tree-ring sensitivity to climate, and emissions from car  
6 traffic may also alter the tree-ring stable isotope signals (Saurer et al., 2004; Leonelli et al., 2012). The species-specific  
7 physiological responses of tree growth to climate variability may be non-linear when high summer temperatures and low soil  
8 moistures exceed specific physiological thresholds, and can interrupt tree-ring growth during the growing season in  
9 Mediterranean climates (Cherubini et al., 2003). In terms of ecological factors, the recurrent attacks of defoliator insects (e.g.,  
10 the pine processionary moth; Hódar et al., 2003), the occurrence of forest fires (e.g., San-Miguel-Ayanz et al., 2013) or herbivory  
11 grazing and land abandonment (Herrero et al., 2011; Camarero and Gutiérrez, 2004) may influence vegetation dynamics and tree  
12 growth in Mediterranean forests, thus potentially introducing non-climatic effects into the chronologies.

13

14 Our reconstruction of the late summer temperature based on conifer MXD shows a clear stable climatic signal over time, and we  
15 could define the spatial coherence of the temperature reconstruction, thus allowing for the determination of the regions that  
16 could be included to extend the reconstruction further back in time. The late-summer temperature reconstruction of Trouet  
17 (2014) is more valid for the region comprising the southern and inner Balkans; our reconstruction is the first fully coherent late  
18 summer temperature reconstruction for Mediterranean Italy, extending in a west-east direction from Sardinia and Sicily to the  
19 Western Balkan area. This spatial approach allows for the definition of areas responding to climatic forcing in homogenous  
20 ways, which may also help predict the forest response to future climate change in the Mediterranean region.

## 21 **5 Conclusion**

22 The climate sensitivity analysis of a multispecies RW and MXD tree-ring network from the Italian Peninsula reveals that conifer  
23 MXD chronologies record a strong and stable signal of late summer temperatures and, to a lesser extent, of summer precipitation  
24 and drought. In contrast, the signals recorded by both conifer and broadleaf RW chronologies are less stable over time but are  
25 still linked to the summer climates of the year prior to growth (conifer) and the year of growth (broadleaves).

26 The reconstruction of the late summer temperatures over the past 300 yr (up to 1980 CE), based on the conifer MXD  
27 chronologies, reveals a strong coherence with the reconstruction performed by Trouet (2014) for the northeastern Mediterranean-  
28 Balkan region, even though the temperatures reconstructed in our study are less variable, likely because all of our sites are  
29 located along the Italian Peninsula and are relatively close to the sea. According to our reconstruction, 1699, 1740, 1814, 1909  
30 and 1939 were years of particularly low late summer temperatures over the study region, whereas the highest temperature was  
31 found approximately 1945. The reconstruction is representative of a wide area covering the Italian Peninsula, Sardinia, Sicily and  
32 the Balkan area close to the Adriatic Sea, which are areas that could be considered to further enhance the regional reconstruction  
33 we performed and to better assess climate change impacts on forests in homogenous areas within the Mediterranean hot spot.

34

35 **Data availability.** Data will be set on the NEXTDATA database (<http://geomatic.disat.unimib.it/paleodata> - a doi: will be  
36 provided).

37

38 **Competing interests.** The authors declare that they have no conflict of interest.

39

40 **Acknowledgements.** This study was funded by the project of strategic interest NEXTDATA (PNR National Research



1 Programme 2011-2013; project coordinator A. Provenzale CNR-IGG, WP leader V. Maggi UNIMIB and CNR-IGG), and by the  
 2 following PRIN 2010-2011 projects (MIUR - Italian Ministry of Education, Universities and Research): grant no.  
 3 2010AYKTAB\_006 (national leader C. Baroni), and grant no. B21J12000560001 'CARBOTREES'.  
 4 This study is also linked to activities conducted within the following COST Actions (European Cooperation in Science and  
 5 Technology), financially supported by the EU Framework Programme for Research and Innovation HORIZON 2020: FP1106  
 6 'STReSS' (Studying Tree Responses to extreme Events: a SynthesiS), and CA15226 CLIMO (Climate-Smart Forestry in  
 7 Mountain Regions). We acknowledge the E-OBS dataset from the EU-FP6 project ENSEMBLES ([http://ensembles-](http://ensembles-eu.metoffice.com)  
 8 [eu.metoffice.com](http://ensembles-eu.metoffice.com)) and the data providers in the ECA&D project (<http://www.ecad.eu>). We thank the several researchers who  
 9 uploaded their raw data onto the ITRDB.

10

11 **References**

12

13 Akkemik, Ü., and Aras A.: Reconstruction (1689–1994 AD) of April–August precipitation in the southern part of central Turkey.  
 14 Int. J. Climatol., 25(4), 537–548, 2005.

15 Akkemik, Ü., D'Arrigo, R., Cherubini, P., Köse, N., and Jacoby, G.C.: Tree-ring reconstructions of precipitation and streamflow  
 16 for north-western Turkey. Int. J. Climatol., 28, 173–183, doi:10.1002/joc.1522, 2008.

17 Babst, F., Poulter, B., Trouet, V., Tan, K., Neuwirth, B., Wilson, R., Carrer, M., Grabner, M., Tegel, W., Levanic, T., Panayotov,  
 18 M., Urbinati, C., Bouriaud, O., Ciais P., and Frank D.: Site- and species-specific responses of forest growth to climate  
 19 across the European continent. Global Ecol. Biogeogr. 22, 706–717, 2013.

20 Barbati, A., Corona, P., and Marchetti, M.: A forest typology for monitoring sustainable forest management: The case of  
 21 European forest types. Plant Biosyst., 141, 93–103, 2007.

22 Battipaglia, G., Saurer, M., Cherubini, P., Siegwolf, R.T.W., and Cotrufo, M.F.: Tree rings indicate different drought resistance of  
 23 a native (*Abies alba* Mill.) and a nonnative (*Picea abies* (L.) Karst.) species co-occurring at a dry site in Southern Italy.  
 24 Forest Ecol. Manag., 257, 820–828, 2009.

25 Battipaglia, G., Frank, D., Büntgen, U., Dobrovolný, P., Brázdil, R., Pfister, C., and Esper, J.: Five centuries of Central European  
 26 temperature extremes reconstructed from tree-ring density and documentary evidence. Global Planet. Change, 72, 182–191,  
 27 2010.

28 Becker, B.: An 11,000-year German oak and pine dendrochronology for radiocarbon calibration. Radiocarbon 35(1), 201-213,  
 29 1993.

30 Biondi, F.: Comparing tree-ring chronologies and repeated timber inventories as forest monitoring tools. Ecol. Appl., 9, 216–  
 31 227, 1999.

32 Biondi, F., and Waikul, K.: DENDROCLIM2002: a C++ program for statistical calibration of climate signals in tree-ring  
 33 chronologies. Comput. Geosci., 30, 303–311, 2004.

34 Boisvenue, C., and Running, S.W.: Impacts of climate change on natural forest productivity – evidence since the middle of the  
 35 20th century. Glob. Change Biol., 12, 862–882, 2006.

36 Boydak, M., and Dogru, M.: The exchange of experience and state of the art in sustainable forest management (SFM) by  
 37 ecoregion: Mediterranean forests. Ecoregional review. In: Proceedings of the XI World Forestry Congress, 13-22 October  
 38 1997, Antalya, 6, 179–204, 1997.

39 Borghetti, M., Gentilesca, T., Leonardi, S., van Noije, T., and Rita, A.: Long-term temporal relationships between environmental  
 40 conditions and xylem functional traits: a meta-analysis across a range of woody species along climatic and nitrogen  
 41 deposition gradients. Tree Physiol., doi:10.1093/treephys/tpw087, in press 2016.

42 Brienens, R.J.W., Gloor, E., and Zuidema, P.: Detecting evidence for CO<sub>2</sub> fertilization from tree ring studies: The potential role of



- 1 sampling biases. *Global Biogeochem. Cy.*, 26, GB1025, doi:10.1029/2011GB004143, 2012.
- 2 Briffa, K.R., Jones, P.D., Pilcher, J.R., and Hughes, M.K.: Reconstructing summer temperatures in Northern Fennoscandia back  
3 to A.D. 1700 using tree-ring data from scots pine. *Arct. Antarct. Alp. Res.* 20, 385–394, 1988.
- 4 Briffa, K.R., and Jones, P.D.: Basic chronology statistics and assessment. In: E. R. Cook, and L. A. Kairiukstis (Eds.), *Methods*  
5 *of Dendrochronology: Applications in the Environmental Sciences: 137–152.* Kluwer, Dordrecht, The Netherlands, 1990.
- 6 Briffa, K.R., Jones, P.D., Bartholin, T.S., Eckstein, D., Schweingruber, F.H., Karlén, W., Zetterberg, P., and Eronen, M.:  
7 Fennoscandian summers from AD 500: temperature changes on short and long timescales. *Clim. Dynam.*, 7, 111–119,  
8 1992.
- 9 Briffa, K.R., Osborn, T.J., and Schweingruber, F.H.: Large-scale temperature inferences from tree rings: a review. *Global Planet.*  
10 *Change*, 40, 11–26, 2004.
- 11 Briffa, K.R., and Melvin, T.M.: A closer look at regional curve standardisation of tree-ring records: justification of the need, a  
12 warning of some pitfalls, and suggested improvements in its application. In: Diaz HF, Swetnam TW (eds) Hughes MK.  
13 *Dendroclimatology, Progress and Prospects.* Springer Verlag, pp. 113–145, 2011.
- 14 Brunetti, M., Maugeri, M., Monti, F., and Nanni, T.: Temperature and precipitation variability in Italy in the last two centuries  
15 from homogenised instrumental time series. *Int. J. Climatol.*, 26, 345–381, 2006.
- 16 Brunetti, M., Lentini, G., Maugeri, M., Nanni, T., Simolo, C., and Spinoni, J.: Projecting North Eastern Italy temperature and  
17 precipitation secular records onto a high resolution grid. *Phys. Chem. Earth*, 40–41, 9–22, doi:10.1016/j.pce.2009.12.005,  
18 2012.
- 19 Brunetti, M., Maugeri, M., Nanni, T., Simolo, C., and Spinoni, J.: High-resolution temperature climatology for Italy:  
20 interpolation method intercomparison. *Int. J. Climatol.*, 34, 1278–1296, doi:10.1002/joc.3764, 2014.
- 21 Büntgen, U., Frank, D.C., Schmidhalter, M., Neuwirth, B., Seifert, M., and Esper, J.: Growth/climate response shift in a long  
22 subalpine spruce chronology. *Trees*, 20, 99–110, doi:10.1007/s00468-005-0017-3, 2006.
- 23 Büntgen, U., Frank, D., Trouet, V., and Esper, J.: Diverse climate sensitivity of Mediterranean tree-ring width and density. *Trees*,  
24 24, 261–273, doi 10.1007/s00468-009-0396-y, 2010
- 25 Calfapietra, C., Barbati, A., Perugini, L., Ferrari, B., Guidolotti, G., Quatrini, A., and Corona, P.: Carbon stocks and potential  
26 carbon sequestration of different forest ecosystems under climate change and various management regimes in Italy.  
27 *Ecosyst. Health Sustain.*, 1(8), 25, doi:10.1890/EHS15-0023, 2015.
- 28 Camarero, J.J. and Gutiérrez, E.: Pace and pattern of recent treeline dynamics: response of ecotones to climatic variability in the  
29 Spanish Pyrenees. *Climatic Change*, 63, 181–200, 2004.
- 30 Carrer, M., Nola, P., Motta, R., and Urbinati, C.: Contrasting tree-ring growth to climate responses of *Abies alba* toward the  
31 southern limit of its distribution area. *Oikos*, 119, 1515–1525, doi:10.1111/j.1600-0706.2010.18293.x, 2010.
- 32 Castagneri, D., Nola, P., Motta, R., and Carrer, M.: Summer climate variability over the last 250 years differently affected tree  
33 species radial growth in a mesic *Fagus–Abies–Picea* old-growth forest. *Forest Ecol. Manag.*, 320, 21–29, 2014.
- 34 Cherubini, P., Gartner, B.L., Tognetti, R., Bräker, O.U., Schoch, W., and Innes, J.L.: Identification, measurement and  
35 interpretation of tree rings in woody species from Mediterranean climates. *Biol. Rev.*, 78, 119–148,  
36 doi:10.1017/S1464793102006000, 2003.
- 37 Coppola, A., Leonelli, G., Salvatore, M.C., Pelfini, M., and Baroni, C.: Weakening climatic signal since mid-20th century in  
38 European larch tree-ring chronologies at different altitudes from the Adamello-Presanella Massif (Italian Alps). *Quaternary*  
39 *Res.*, 77, 344–354, doi:10.1016/j.yqres.2012.01.004, 2012.
- 40 Corpo Forestale dello Stato: Secondo inventario nazionale delle foreste e dei serbatoi forestali di carbonio (INFC 2005).  
41 Available at <http://www.sian.it> (site consulted on September 2016), 2005.
- 42 Crespi, A., Brunetti, M., Lentini, G., and Maugeri, M.: 1961–1990 high-resolution monthly precipitation climatologies for Italy".



- 1 Int. J. Climatol., submitted, 2017.
- 2 Dafis, S.: The Mediterranean Forest and its protection. *Sci. Ann. Dept. Forest. Nat. Environ.*, 37, 159–170, 1997.
- 3 Elling, W., Dittmar, C., Pfaffelmoser, K., and Roetzer, T.: Dendroecological assessment of the complex causes of decline and  
4 recovery of the growth of silver fir (*Abies alba* Mill.) in Southern Germany. *For. Ecol. Manage.*, 257, 1175–1187, 2009.
- 5 Esper, J., Cook, E.R., Krusic, P.J., Peters, K., and Schweingruber, F.H.: Tests of the RCS method for preserving low frequency  
6 variability in long tree-ring chronologies. *Tree-Ring Res.*, 59, 81–98, 2003.
- 7 Esper, J., Frank, D.C., Wilson, R.J.S., and Briffa, K.R.: Effect of scaling and regression on reconstructed temperature amplitude  
8 for the past millennium. *Geophys. Res. Lett.*, 32, L07711, doi:10.1029/2004GL021236, 2005.
- 9 Esper, J., Frank, D., Büntgen, U., and Kirilyanov, A.: Influence of pith offset on tree-ring chronology trend. In: Kaczka, R.,  
10 Malik, I., Owczarek, P., Gärtner, H., Helle, G., Heinrich, I. (eds) TRACE - Tree Rings in Archaeology, Climatology and  
11 Ecology Vol. 7. GFZ Potsdam, Scientific Technical Report STR 09/03, Potsdam, pp. 205–210, 2009.
- 12 Friedrich, M., Remmele, S., Kromer, B., Hofmann, J., Spurk, M., Kaiser, K.F., Orsel, C., and Küppers, M.: The 12,460-year  
13 Hohenheim oak and pine tree-ring chronology from central Europe — a unique annual record for radiocarbon calibration  
14 and paleoenvironment reconstructions. *Radiocarbon*, 46(3), 1111–1122, 2004.
- 15 Fritts, H.C.: *Tree rings and climate*. Academic Press, New York, 1976
- 16 Galván, J.D., Camarero, J.J., Ginzler, C., and Büntgen, U.: Spatial diversity of recent trends in Mediterranean tree growth.  
17 *Environ. Res. Lett.* 9, 084001, doi:10.1088/1748-9326/9/8/084001, 2014.
- 18 Galván, J.D., Büntgen, U., Ginzler, C., Grudd, H., Gutiérrez, E., Labuhn, I., and Camarero, J.J.: Drought-induced weakening of  
19 growth–temperature associations in high-elevation Iberian pines. *Global Planet. Change*, 124, 95–106, 2015.
- 20 Giorgi, F.: Climate change hot-spots. *Geophys. Res. Lett.*, 33, L08707, doi:10.1029/2006gl025734, 2006.
- 21 Griggs, C., DeGaetano, A., Kuniholm, P., and Newton, M.: A regional high-frequency reconstruction of May–June precipitation  
22 in the north Aegean from oak tree rings, A.D. 1809–1989. *Int. J. Clim.*, 27, 1075–1089, 2007.
- 23 Haylock, M.R., Hofstra, N., Klein Tank, A.M.G., Klok, E.J., Jones, P.D., and New, M.: A European daily high-resolution gridded  
24 dataset of surface temperature and precipitation. *J. Geophys. Res.*, 113, D20119, doi:10.1029/2008JD10201, 2008.
- 25 Herrero, A., Zamora, R., Castro, J., and Hódar, J.A.: Limits of pine forest distribution at the treeline: herbivory matters. *Plant*  
26 *Ecol.*, 213, 459–469, 2011.
- 27 Hódar, J.A., Castro, J., and Zamora, R.: Pine processionary caterpillar *Thaumetopoea pityocampa* as a new threat for relict  
28 Mediterranean Scots pine forests under climatic warming. *Biol. Conserv.*, 110, 123–129, 2003.
- 29 IPCC: Climate Change 2013. The Physical Science Basis. Contribution of Working Group I to the Fifth Assessment Report of  
30 the Intergovernmental Panel on Climate Change. Stocker, T.F., D. Qin, G.-K. Plattner, M. Tignor, S.K. Allen, J. Boschung,  
31 A. Nauels, Y. Xia, V. Bex and P.M. Midgley (eds.). Cambridge University Press, Cambridge, United Kingdom and New  
32 York, NY, USA, 1535 pp, doi:10.1017/CBO9781107415324, 2013.
- 33 Jacoby, G.C., and D’Arrigo, R.D.: Tree rings, carbon dioxide, and climatic change. *Proc. Natl. Acad. Sci. USA* 94, 8350–8353,  
34 1997.
- 35 Kern, Z., Popa, I., Varga, Z., and Széles, É.: Degraded temperature sensitivity of a stone pine chronology explained by  
36 dendrochemical evidences. *Dendrochronologia*, 27, 121–128, 2009.
- 37 Körner, C.: Carbon limitation in trees. *J. Ecol.*, 91, 4–17, 2003.
- 38 Köse, N., Akkemik, Ü., Dalfes, H. N., and Özeren, M. S.: Tree-ring reconstructions of May–June precipitation of western  
39 Anatolia. *Quaternary Res.*, 75, 438–450, 2011.
- 40 Köse, N., Akkemik Ü., Güner H.T., Dalfes H.N., Grissino-Mayer H.D., Özeren M.S., and Kindap T.: An improved  
41 reconstruction of May–June precipitation using tree-ring data from western Turkey and its links to volcanic eruptions. *Int.*  
42 *J. Biometeorol.*, 57, 691–701, doi:10.1007/s00484-012-0595-x, 2013.



- 1 Köse, N., Güner, H.T., Harley, G.L., and Guiot, J.: Spring temperature variability over Turkey since 1800 CE reconstructed from  
2 a broad network of tree-ring data. *Clim. Past*, 13, 1–15, doi:10.5194/cp-13-1-2017, 2017.
- 3 Lebourgeois, F., Merian, P., Courdier, F., Ladier, J., and Dreyfus, P.: Instability of climate signal in tree-ring width in  
4 Mediterranean mountains: a multi-species analysis. *Trees-Struct. Funct.*, 26, 715–729, 2012.
- 5 Leonelli, G., Pelfini, M., Battipaglia, G., and Cherubini, P.: Site-aspect influence on climate sensitivity over time of a high-  
6 altitude *Pinus cembra* tree-ring network. *Climatic Change*, 96(1-2), 185–201, doi:10.1007/s10584-009-9574-6, 2009.
- 7 Leonelli, G., Battipaglia, G., Siegwolf, R.T.W., Saurer, M., Morra di Cella, U., Cherubini, P., and Pelfini, M.: Climatic isotope  
8 signals in tree rings masked by air pollution: A case study conducted along the Mont Blanc Tunnel access road (Western  
9 Alps, Italy). *Atmos. Environ.*, 61, 169–179, 2012.
- 10 Leonelli, G., Coppola, A., Baroni, C., Salvatore, M.C., Maugeri, M., Brunetti, M., and Pelfini, M.: Multispecies dendroclimatic  
11 reconstructions of summer temperature in the European Alps enhanced by trees highly sensitive to temperature. *Climatic  
12 Change*, 137, 275–291, doi:10.1007/s10584-016-1658-5, 2016.
- 13 Levanič, T., Popa, I., Poljanšek, S., and Nechita, C.: A 323-year long reconstruction of drought for SW Romania based on black  
14 pine (*Pinus nigra*) tree-ring widths. *Int. J. Biometeorol.*, 57(5), 703–714, 2013.
- 15 Marchetti, M., Tognetti, R., Lombardi, F., Chiavetta, U., Palumbo, G., Sellitto, M., Colombo, C., Iovieno, P., Alfani, A.,  
16 Baldantoni, D., Barbati, A., Ferrari, B., Bonacquisti, S., Capotorti, G., Copiz, R., and Blasi, C.: Ecological portrayal of old-  
17 growth forests and persistent woodlands in the Cilento and Vallo di Diano National Park (southern Italy). *Plant Biosystems*,  
18 144, 130–147, 2010.
- 19 Martin-Benito, D., Beeckman, H., and Cañellas, I.: Influence of drought on tree rings and tracheid features of *Pinus nigra* and  
20 *Pinus sylvestris* in a mesic Mediterranean forest. *Eur. J. Forest Res.*, 132, 33–45, doi 10.1007/s10342-012-0652-3, 2013.
- 21 Martin-Benito, D., Ummenhofer C.C., Köse N., Güner H.T., and Pederson, N.: Tree-ring reconstructed May–June precipitation  
22 in the Caucasus since 1752 CE. *Clim. Dyn.*, 47, 3011–3027, doi:10.1007/s00382-016-3010-1, 2016.
- 23 McKee, T.B., Doesken, N.J., and Kleist, J.: Drought monitoring with multiple time scales. Ninth Conference on Applied  
24 Climatology, American Meteorological Society, Jan15-20, 1995, Dallas TX, pp.233–236, 1995.
- 25 Mitchell, T.D., and Jones, P.D.: An improved method of constructing a database of monthly climate observations and associated  
26 high-resolution grids. *Int. J. Climatol.*, 25(6), 693–712, 2005.
- 27 New, M., Hulme, M., and Jones, P.: Representing twentieth-century space-time climate variability. Part II: Development of  
28 1901–96 monthly grids of terrestrial surface climate. *J. Climate*, 13, 2217–2238, 2000.
- 29 Nicault, A., Alleaume, S., Brewer, S., Carrer, M., Nola, P., and Guiot, J.: Mediterranean drought fluctuation during the last 500  
30 years based on tree-ring data. *Clim. Dyn.*, 31, 227–245, doi:10.1007/s00382-007-0349-3, 2008.
- 31 Nicolussi, K., Kaufmann, M., Melvin, T.M., van der Plicht, J., Schießling, P., and Thurner, A.: A 9111 year long conifer tree-ring  
32 chronology for the European Alps: a base for environmental and climatic investigations. *Holocene*, 19(6), 909–920,  
33 doi:10.1177/0959683609336565, 2009.
- 34 Palacio, S., Hoch, G., Sala, A., Körner, C., and Millard, P.: Does carbon storage limit tree growth? *New Phytol.*, 201, 1096–1100,  
35 2013.
- 36 Palmer, W.C.: Meteorological drought. US Weather Bureau. Research paper n 45, Washington DC, 58 p, 1965.
- 37 Pelfini, M., Leonelli, G., and Santilli, M.: Climatic and environmental influences on mountain pine (*Pinus montana* Miller)  
38 growth in the Central Italian Alps. *Arct. Antarct. Alp. Res.*, 38(4), 614–623, 2006.
- 39 Piovesan, G., and Schirone, B.: Winter North Atlantic oscillation effects on the tree rings of the Italian beech (*Fagus sylvatica*  
40 L.). *Int. J. Biometeorol.*, 44, 121–127, 2000.
- 41 Piovesan, G., Biondi, F., Bernabei, M., Di Filippo, A., and Schirone, B.: Spatial and altitudinal bioclimatic zones of the Italian  
42 peninsula identified from a beech (*Fagus sylvatica* L.) tree-ring network. *Acta Oecol.*, 27, 197–210, 2005.



- 1 Piovesan, G., Biondi, F., Di Filippo, A., Alessandrini, A., and Maugeri, M.: Drought-driven growth reduction in old beech  
2 (*Fagus sylvatica* L.) forests of the central Apennines, Italy. *Glob. Change Biology*, 14, 1–17, doi:10.1111/j.1365-  
3 2486.2008.01570.x, 2008.
- 4 Ripullone, F., Borghetti, M., Raddi, S., Baraldi, R., Nolè, A., Guerrieri, M.R., and Magnani, F.: Physiological and structural  
5 changes in response to altered precipitation regime in an evergreen Mediterranean macchia. *Trees-Struct. Funct.*, 23, 823–  
6 834, 2009.
- 7 Rita, A., Gentilella, T., Ripullone, F., Todaro, L., and Borghetti, M.: Differential climate-growth relationships in *Abies alba* Mill.  
8 and *Fagus sylvatica* L. in Mediterranean mountain forests. *Dendrochronologia*, 32, 220–229, 2014.
- 9 Ruiz-Labourdette, D., Génova, M., Schmitz, M.F., Urrutia, R., and Pineda, F.D.: Summer rainfall variability in European  
10 Mediterranean mountains from the sixteenth to the twentieth century reconstructed from tree rings. *Int. J. Biometeorol.*, 58,  
11 1627–1639, doi:10.1007/s00484-013-0766-4, 2014
- 12 Rutherford, S.D., Mann, M.E., Osborn, T.J., Bradley, R.S., Briffa, K.R., Hughes, M.K., and Jones, P.D.: Proxy-based Northern  
13 Hemisphere surface temperature reconstructions: sensitivity to method, predictor network, target season and target domain.  
14 *J. Climate*, 18, 2308–2329, 2005.
- 15 Saurer, M., Cherubini, P., Ammann, M., De Cinti, B., and Siegwolf, R.T.W.: First detection of nitrogen from NO<sub>x</sub> in tree rings: a  
16 <sup>15</sup>N/<sup>14</sup>N study near a motorway. *Atmos. Environ.*, 38, 2779–2787, 2004.
- 17 Sala, O.E., et al.: Global Biodiversity Scenarios for the Year 2100. *Science*, 287, 1770–1774, 2000.
- 18 San-Miguel-Ayán, J., Moreno, J.M., and Camia, A.: Analysis of large fires in European Mediterranean landscapes: Lessons  
19 learned and perspectives. *Forest Ecol. Manag.*, 294, 11–22, 2013.
- 20 Scarascia-Mugnozza, G., and Matteucci, G.: The impact of temperature and drought on the carbon balance of forest ecosystems:  
21 the case of a beech forest in central Italy. *Agrochimica*, 58, 34–39, 2014.
- 22 Schröter, D., et al.: Ecosystem service supply and vulnerability to global change in Europe. *Science*, 313, 1333–1337, 2005.
- 23 Seim, A., et al.: Climate sensitivity of Mediterranean pine growth reveals distinct east–west dipole. *Int. J. Climatol.*, 35, 2503–  
24 2513, 2015.
- 25 Sensula, B., Wilczyński, S., and Opała, M.: Tree growth and climate relationship: dynamics of Scots pine (*Pinus sylvestris* L.)  
26 growing in the near-source region of the combined heat and power plant during the development of the pro-ecological  
27 strategy in Poland. *Water Air Soil Pollut.*, 226, 220, doi:10.1007/s11270-015-2477-4, 2015.
- 28 Simolo, C., Brunetti, M., Maugeri, M., Nanni, T., and Speranza, A.: Understanding climate change-induced variations in daily  
29 temperature distributions over Italy. *J. Geophys. Res.*, 115, D22110, doi:10.1029/2010JD014088, 2010.
- 30 Somot, S., Sevault, F., Déqué, M., and Crépon, M.: 21<sup>st</sup> century climate change scenario for the Mediterranean using a coupled  
31 atmosphere-ocean regional climate model. *Global Planet. Change*, 63, 112–126, 2007.
- 32 Tejedor, E., de Luis, M., Cuadrat, J.M., Esper, J., and Saz, M.A.: Tree-ring-based drought reconstruction in the Iberian Range  
33 (east of Spain) since 1694. *Int. J. Biometeorol.*, 60, 361–372, doi:10.1007/s00484-015-1033-7, 2016.
- 34 Tessier, L., Nola, P., and Serre-Bachet, F.: Deciduous *Quercus* in the Mediterranean region: tree-ring/climate relationships. *New  
35 Phytol.*, 126, 355–367, 1994.
- 36 Todaro, T., Andreu, L., D’Alessandro, C.M., Gutiérrez, E., Cherubini P., and Saracino A.: Response of *Pinus leucodermis* to  
37 climate and anthropogenic activity in the National Park of Pollino (Basilicata, Southern Italy). *Biol. Cons.*, 137, 507–519,  
38 2007.
- 39 Touchan, R., Meko, D., and Hughes, M.K.: A 396-year reconstruction of precipitation in Southern Jordan. *J. Am. Water Resour.  
40 As.*, 35, 49–59, 1999.
- 41 Touchan, R., Xoplaki, E., Funchouser, G., Luterbacher, J., Hughes, M.K., Erkan, N., Akkemik, U., and Stephan, J.:  
42 Reconstruction of spring/summer precipitation for the Eastern Mediterranean from tree-ring widths and its connection to



- 1 large-scale atmospheric circulation. *Climate Dyn.*, 25, 75–98, 2005a.
- 2 Touchan, R., Funkhouser, G., Hughes, M.K., and Erkan, N.: Standardized precipitation index reconstructed from Turkish ring  
3 widths. *Climatic Change*, 72, 339–353, 2005b.
- 4 Touchan, R., Shishov, V.V, Tychkov, I.I., Sivrikaya, F., Attieh, J., Ketmen, M., Stephan, J., Mitsopoulos, I., Christou, A., and  
5 Meko, D.M.: Elevation-layered dendroclimatic signal in eastern Mediterranean tree rings. *Environ. Res. Lett.*, 11, 044020,  
6 doi:10.1088/1748-9326/11/4/044020, 2016.
- 7 Touchan, R., et al.: Climate controls on tree growth in the Western Mediterranean. *Holocene*, doi: 10.1177/0959683617693,  
8 2017.
- 9 Trouet, V., and Oldenborgh, G.J. van: KNMI Climate Explorer: a web-based research tool for high-resolution paleoclimatology.  
10 *Tree-Ring Res.*, 69(1), 3–13, 2013.
- 11 Trouet, V.: A tree-ring based late summer temperature reconstruction (AD 1675–1980) for the northeastern Mediterranean.  
12 *Radiocarbon*, 56(4), S69–S78, doi:10.2458/azu\_rc.56.18323, 2014.
- 13 Turco, M., Palazzi, E., von Hardenberg, J., and Provenzale, A.: Observed climate change hot-spots. *Geophys. Res. Lett.*, 42,  
14 doi:10.1002/2015GL063891, 2015.
- 15 Turco, M., von Hardenberg, J, AghaKouchak, A., Llasat, M.C., Provenzale, A., and Trigo, R.M.: On the key role of droughts in  
16 the dynamics of summer fires in Mediterranean Europe. *Nature*, *in press* 2017.
- 17 Vicente-Serrano, S.M., Beguería, S., and López-Moreno, J.I.: A multiscalar drought index sensitive to global warming: the  
18 standardized precipitation evapotranspiration index. *J. Clim.*, 23(7), 1696–718, 2010.
- 19 Wigley, T.M.L., Briffa, K.R., and Jones, P.D.: On the average value of correlated time series, with applications in  
20 dendroclimatology and hydrometeorology. *J. Clim. Appl. Meteorol.*, 23, 201–213, 1984.
- 21 WMO, World Meteorological Organization: Standardized Precipitation Index - User Guide. No. 1090. ISBN 978-92-63-11091-6,  
22 2012.
- 23



1 **Table 1:** References for all the dendrochronological data used in this research, information on site locations, types of parameter  
2 used at each site and the tree species. Sites are ordered along a decreasing latitudinal gradient, after differentiating between  
3 conifers and broadleaves (dotted line).

4

Dataset name	Database Source	Original contributor	Database information and site location					Type of tree-ring parameter			
			Bibliographic reference	Location Name	Latitude N	Longitude E	Elevation (m a.s.l.)	RW chr.	RW series	MXD chr.	Species
ITRDBITAL017	ITRDB	Ori, G.G.	<a href="https://www.ncdc.noaa.gov/paleo/study/4079">https://www.ncdc.noaa.gov/paleo/study/4079</a>	Monte Cantiere	44° 16' 48"	10° 48' 00"	800	x			<i>Pinus sp.</i>
ITRDBITAL009	ITRDB	Schweingruber, F.H.	<a href="https://www.ncdc.noaa.gov/paleo/study/4301">https://www.ncdc.noaa.gov/paleo/study/4301</a>	Abetone	44° 07' 12"	10° 42' 00"	1400		x	x	<i>Abies alba</i>
ITRDBITAL004	ITRDB	Biondi, F.	<a href="https://www.ncdc.noaa.gov/paleo/study/2753">https://www.ncdc.noaa.gov/paleo/study/2753</a>	Campolino	44° 06' 45"	10° 39' 44"	1650		x		<i>Picea abies</i>
ITRDBITAL008	ITRDB	Schweingruber, F.H.	<a href="https://www.ncdc.noaa.gov/paleo/study/4540">https://www.ncdc.noaa.gov/paleo/study/4540</a>	Mount Falterona	43° 52' 12"	11° 40' 12"	1450	x		x	<i>Abies alba</i>
ITRDBITAL003	ITRDB	Biondi, F.	<a href="https://www.ncdc.noaa.gov/paleo/study/2760">https://www.ncdc.noaa.gov/paleo/study/2760</a>	Pineta San Rossore	43° 43' 12"	10° 18' 00"	5	x			<i>Pinus pinea</i>
ITRDBITAL022	ITRDB	Becker, B.	<a href="https://www.ncdc.noaa.gov/paleo/study/2706">https://www.ncdc.noaa.gov/paleo/study/2706</a>	Pratomagno Bibbiena - Appennini	43° 40' 12"	11° 46' 12"	1050		x		<i>Abies sp.</i>
ITRDBITAL012	ITRDB	Schweingruber, F.H.	<a href="https://www.ncdc.noaa.gov/paleo/study/4374">https://www.ncdc.noaa.gov/paleo/study/4374</a>	Ceppo Bosque di Martense	42° 40' 48"	13° 25' 48"	1700	x		x	<i>Abies alba</i>
Abies-Abeti-Soprani	UNIMOL			Colle Canalicchio-Abeti Soprani	41° 51' 40"	14° 17' 51"	1350		x		<i>Abies alba</i>
ITRDBITAL016	ITRDB	Schweingruber, F.H.	<a href="https://www.ncdc.noaa.gov/paleo/study/4536">https://www.ncdc.noaa.gov/paleo/study/4536</a>	Monte Mattone	41° 46' 48"	14° 01' 48"	1550	x		x	<i>Pinus nigra</i>
ITRDBITAL001	ITRDB	Biondi, F.	<a href="https://www.ncdc.noaa.gov/paleo/study/2752">https://www.ncdc.noaa.gov/paleo/study/2752</a>	Camosciara Mt. Amaro	41° 46' 12"	13° 49' 12"	1550	x			<i>Pinus nigra</i>
ITRDBITAL002	ITRDB	Biondi, F.	<a href="https://www.ncdc.noaa.gov/paleo/study/2759">https://www.ncdc.noaa.gov/paleo/study/2759</a>	Parco del Circeo	41° 19' 48"	13° 03' 02"	5	x			<i>Pinus pinea</i>
AAIBA	UNIBAS			Ruoti (PZ)	40° 42' 04"	15° 43' 43"	925		x		<i>Abies alba</i>
ITRDBITAL011	ITRDB	Schweingruber, F.H.	<a href="https://www.ncdc.noaa.gov/paleo/study/4541">https://www.ncdc.noaa.gov/paleo/study/4541</a>	Mount Pollino	39° 54' 00"	16° 12' 00"	1720	x		x	<i>Abies alba</i>
ITRDBITAL015	ITRDB	Schweingruber, F.H.	<a href="https://www.ncdc.noaa.gov/paleo/study/4644">https://www.ncdc.noaa.gov/paleo/study/4644</a>	Sierra de Crispo	39° 54' 00"	16° 13' 48"	2000	x		x	<i>Pinus leucodermis</i> <i>Abies alba</i>
ITRDBITAL010	ITRDB	Schweingruber, F.H.	<a href="https://www.ncdc.noaa.gov/paleo/study/4420">https://www.ncdc.noaa.gov/paleo/study/4420</a>	Gambarie Aspromonte	38° 10' 12"	15° 55' 12"	1850	x		x	<i>Abies alba</i>
ITRDBITAL013	ITRDB	Schweingruber, F.H.	<a href="https://www.ncdc.noaa.gov/paleo/study/4304">https://www.ncdc.noaa.gov/paleo/study/4304</a>	AetnaLinguaglossa	37° 46' 48"	15° 03' 00"	1800	x		x	<i>Pinus nigra</i>
ITRDBITAL019	ITRDB	Nola, P.	<a href="https://www.ncdc.noaa.gov/paleo/study/4002">https://www.ncdc.noaa.gov/paleo/study/4002</a>	Corte Brugnatella	44° 43' 12"	09° 19' 12"	900	x			<i>Quercus robur</i>
Fagus-Parco-Abruzzo	UNIMOL			Vai Cervara	41° 49' 00"	13° 43' 00"	1780		x		<i>Fagus sylvatica</i>
Fagus-Gargano	UNIMOL			Parco Nazionale del Gargano Riserva Pavari	41° 49' 00"	16° 00' 00"	775		x		<i>Fagus sylvatica</i>
Fagus-Montedimezzo	UNIMOL			Riserva MaB Unesco Collemeluccio-Montedimezzo	41° 45' 00"	14° 12' 00"	1100	x			<i>Fagus sylvatica</i>
Cervialto-FASY	UNINA2			Monti Picoentini	40° 50' 23"	15° 10' 03"	800		x		<i>Fagus sylvatica</i>
Fagus-Cliento	UNIMOL			Parco Nazionale del Cliento Ottati	40° 28' 00"	15° 24' 00"	1130		x		<i>Fagus sylvatica</i>
QCIBG	UNIBAS			Gorgoglione (MT)	40° 23' 09"	16° 10' 04"	820		x		<i>Quercus cerris</i>
QFIMP1	UNIBAS			San Paolo Albanese (PZ)	40° 01' 20"	16° 20' 26"	1050	x			<i>Quercus frainetto</i> <i>Quercus frainetto</i>
QFIMP2	UNIBAS			Oriolo (CS)	40° 00' 10"	16° 23' 29"	960	x			<i>Quercus frainetto</i> <i>Fagus sylvatica</i>
Fagus-Sta	UNIMOL			Parco Sta	39° 08' 00"	16° 40' 00"	1680		x		<i>Fagus sylvatica</i>
Fagus-Parco-Aspromonte	UNIMOL			Aspromonte	38° 11' 00"	15° 52' 00"	1560		x		<i>Fagus sylvatica</i>
							1235 mean elevation	15 sites	12 sites	8 sites	

5  
6  
7



1 **Table 2:** Main characteristics of the chronologies used in this research, separating RW (comprised of both broadleaf and conifer  
2 species) and MXD (only conifer species). For each site and parameter, the total number of series available and the number of  
3 series showing a correlation value  $0.2 < r < 0.3$  with the respective master chronology is reported. Gray-shaded areas depict  
4 values that do not exceed the fixed thresholds of  $MIC > 0.3$ ,  $EPS > 0.7$  and a number of series  $> 10$ , determining the exclusion of  
5 the chronology from further analyses. Sites ordered as in Table 1.

6 a = Mean Interseries Correlation of raw series, calculated using the maximum period available at each site.

7 b = Expressed Population signal of indexed series in the common period of 1880-1980.

8 \* series up to 80 yr included.

9 \*\* chronology built with less than 10 series (good EPS).

10 \*\*\* common period with later Start date or earlier End date.

11 \*\*\*\* sites without chronology [...] are not included in the computation.

12

Dataset name	RWseries characteristics							MXD series characteristics on the maximum period available						
	Start date	End date	Time span	MIC <sup>a</sup>	EPS <sup>b</sup>	# series	# series $0.2 < r < 0.3$ vs. master	Start date	End date	Time span	MIC1	EPS2	# series	# series $0.2 < r < 0.3$ vs. master
ITRDBI TAL017	1856	1989	134	0.43	0.76	14	0	-	-	-	-	-	-	-
ITRDBI TAL009	[1846]	[1980]	[135]	[0.73]	[0.66]	13	0	1846	1980	135	0.76	0.86	21	0
ITRDBI TAL004	[1836]	[1988]	[153]	[0.51]	[0.49]	11	0	-	-	-	-	-	-	-
ITRDBI TAL008	1827	1980	154	0.62	0.70	12	0	1827	1980	154	0.66	0.87	12	0
ITRDBI TAL003*	1861	1988	128	0.51	0.72	9	0	-	-	-	-	-	-	-
ITRDBI TAL022***	[1539]	[1972]	[434]	[0.45]	[0.67]	6	1	-	-	-	-	-	-	-
ITRDBI TAL012	1654	1980	327	0.57	0.85	26	0	1654	1980	327	0.59	0.91	25	0
Abies>Abeti-Soprani*	[1838]	[2005]	[168]	[0.53]	[0.50]	11	0	-	-	-	-	-	-	-
ITRDBI TAL016	1844	1980	137	0.54	0.84	17	0	1844	1980	137	0.43	0.75	15	0
ITRDBI TAL001	1750	1987	238	0.52	0.77	16	0	-	-	-	-	-	-	-
ITRDBI TAL002*	1878	1988	111	0.51	0.72	16	0	-	-	-	-	-	-	-
AAIBA*	[1866]	[2007]	[142]	[0.51]	[0.55]	13	0	-	-	-	-	-	-	-
ITRDBI TAL011	1800	1980	181	0.58	0.85	20	0	1800	1980	181	0.54	0.84	18	0
ITRDBI TAL015	1415	1980	566	0.58	0.95	22	0	1441	1980	540	0.50	0.76	21	0
ITRDBI TAL010	1790	1980	191	0.53	0.76	19	0	1790	1980	191	0.50	0.85	18	0
ITRDBI TAL013	1773	1980	208	0.57	0.88	20	0	1795	1980	186	0.44	0.78	18	0
ITRDBI TAL019	1779	1988	211	0.54	0.82	16	0	-	-	-	-	-	-	-
Fagus-Parco-Abruzzo	[1716]	[2008]	[293]	[0.36]	[0.73]	3	0	-	-	-	-	-	-	-
Fagus-Gargano	[1821]	[2009]	[189]	[0.23]	[0.42]	3	3	-	-	-	-	-	-	-
Fagus-Montedimezzo Cervialto-FASY	1844	2005	162	0.67	0.85	15	0	-	-	-	-	-	-	-
Fagus-Clenio	[1828]	[2003]	[176]	[0.39]	[0.52]	10	0	-	-	-	-	-	-	-
QCIBG*, ***	[1837]	[2007]	[171]	[0.41]	[0.26]	7	1	-	-	-	-	-	-	-
QFIMP1	[1897]	[2013]	[117]	[0.60]	[0.66]	9	0	-	-	-	-	-	-	-
QFIMP2	1851	2013	163	0.50	0.78	34	0	-	-	-	-	-	-	-
Fagus-Sita	1854	2013	160	0.55	0.79	34	0	-	-	-	-	-	-	-
Fagus-Parco-Aspromonte	[1854]	[2009]	[156]	[0.30]	[0.21]	4	3	-	-	-	-	-	-	-
TOTAL	[1874]	[2009]	[136]	[0.27]	[-0.42]	5	2	-	-	-	-	-	-	-
	1785****	1989****	205****	0.55****	0.80****	385	10	1750	1980	231	0.55	0.83	148	0
	mean	mean	mean	mean r	mean EPS	sum (all sites)	sum (all sites)	mean	mean	mean	mean r	mean EPS	sum	sum (all sites)

13

14

15



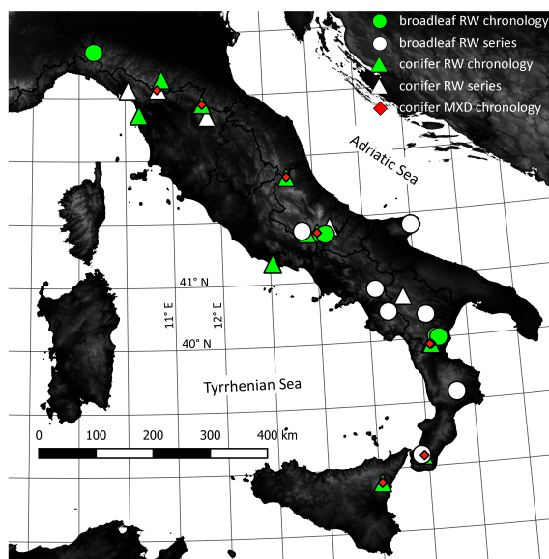
1 **Table 3:** Reconstruction statistics computed for both regressions and scaling over the inverted subperiods of calibration and  
 2 verification. RE = Reduction of error; CE = Coefficient of efficiency.  
 3

		R <sup>2</sup>	Regression		Scaling	
			RE	CE	RE	CE
Calib.	1781-1880	0.377				
Verif	1881-1980		0.472	0.289	0.543	0.384
Calib.	1881-1980	0.510				
Verif	1781-1880		0.390	0.206	0.214	-0.023

4  
5  
6



3



4

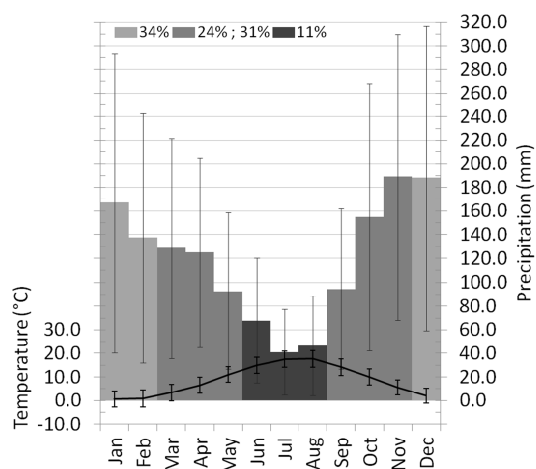
5

0 **Figure 1:** Distribution of the tree-ring sites from central and southern Italy available to the NEXTDATA project and used in  
1 this study. Sites were subdivided by the type of tree (conifer or broadleaf), the type of parameter (RW or MXD) and the  
2 type of data used (site chronology or only tree-ring series).

9



3



4

0

**Figure 2:** Monthly mean temperatures and precipitations over the period of 1880-2014 for all sites considered in this study.

0

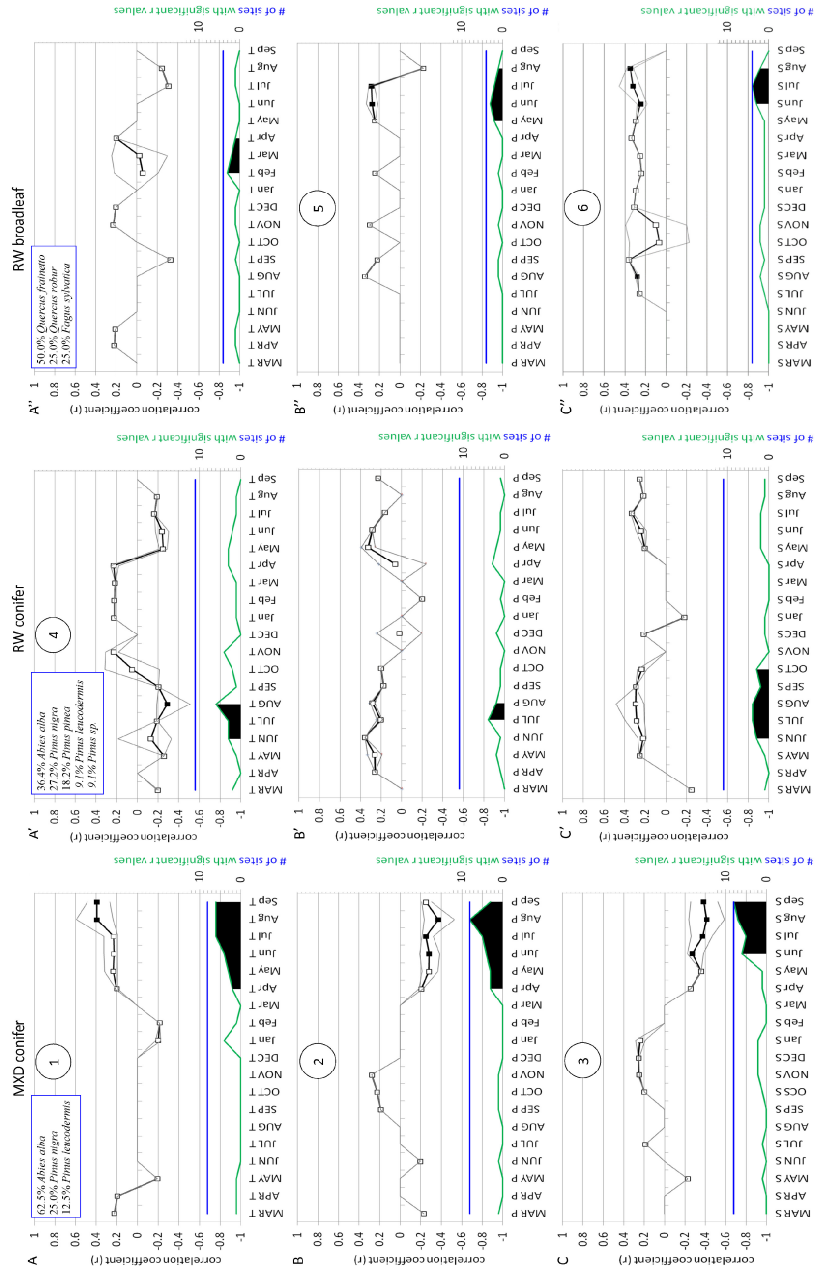
For both temperature and precipitation, the error bars indicate one standard deviation; for precipitation, the seasonal percentages of precipitation with respect to the mean annual value (= 1433 mm) are reported.

1

8



3  
4



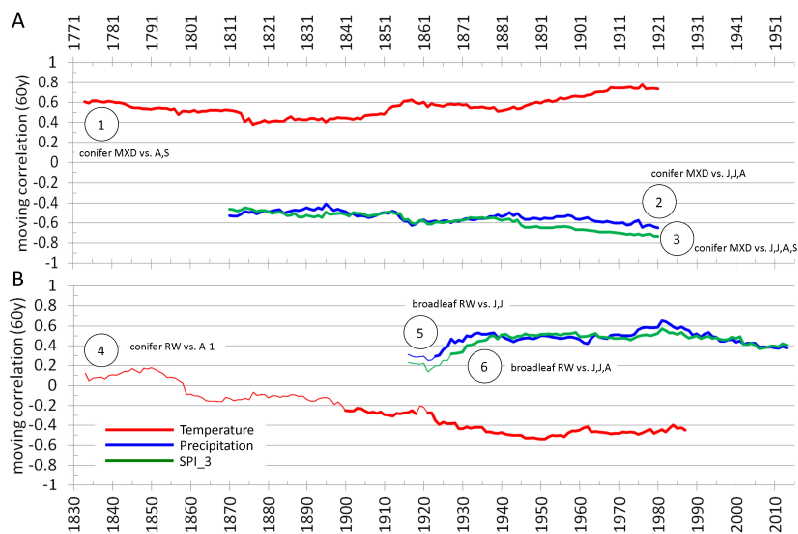
5  
6



1 **Figure 3:** Bootstrapped correlation analysis performed over the common period of 1880-1980, considering chronologies of  
2 conifer MXD (3A, 3B and 3C), of conifer RW (3A', 3B' and 3C') and of broadleaf RW (3A'', 3B'' and 3C'') vs. monthly  
3 temperature (T), precipitation (P) and SPI\_3 (S) from March of the year prior to growth to September of the year of growth.  
4 In A, A' and A'' the percentages of the species composing the pool for each site used for the analysis is reported.  
5 Means of statistically significant ( $p < 0.05$ ) correlation coefficient values ( $r$ ) are depicted with squares, whereas maximum  
6 and minimum significant  $r$  values are indicated with gray lines; the blue lines depict the total number of sites in each  
7 comparison and the green lines indicate the total number of sites with statistically significant  $r$  values. Black-filled squares  
8 are given for those variables that show significant correlation values for at least 50 % of the total sites and have  $|\bar{r}| > 0.25$ ;  
9 where both conditions occur, a circled number in the plot is given and the comparisons are selected for the following  
10 moving correlation analysis (Fig. 4). In each plot the climate variables with the highest number of sites with significant  $r$   
11 values and nearby variables showing up to  $\frac{1}{4}$  of this number are depicted with a black area.  
12



3



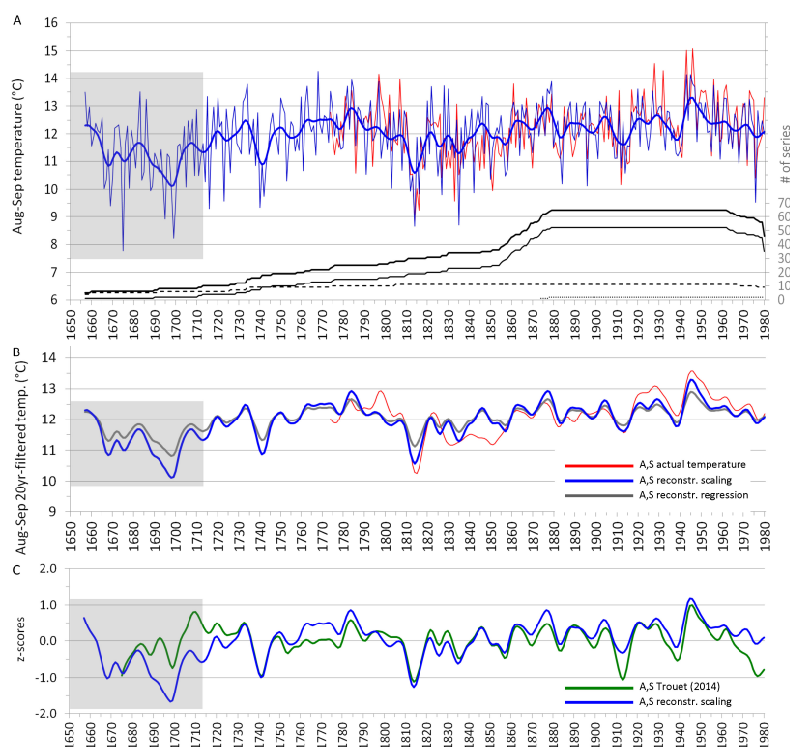
4

1 **Figure 4:** Bootstrapped moving correlation analysis with a 60 yr time window, performed over the maximum period  
 2 available for the HSTC chronologies and their respective climate variables (temperature, precipitation and SPI\_3) selected  
 3 in the previous analysis (circled numbers as in Fig. 3). The statistically significant values ( $p < 0.05$ ) of  $r$  are depicted by bold  
 14 lines.

9



3



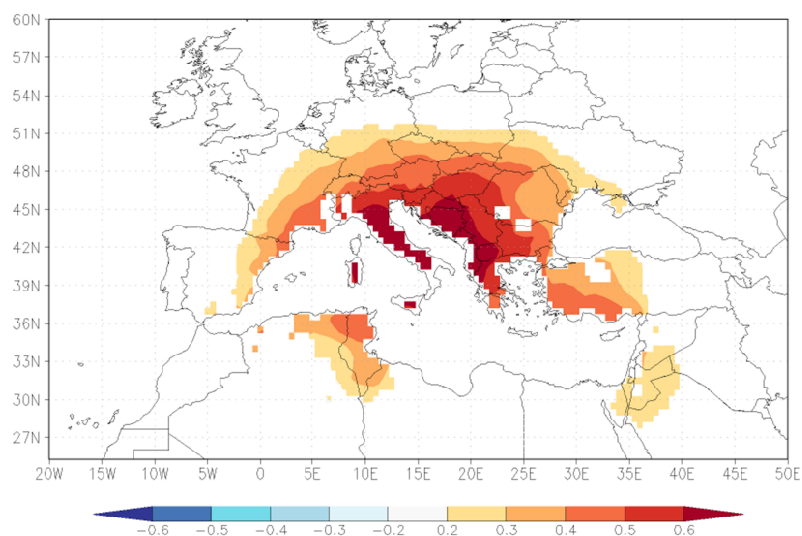
4

19 **Figure 5:** Reconstruction of late summer (August and September) temperature using the conifer MXD chronology with the  
 20 scaling approach for the period 1650-1980 CE (5A). The bold black line indicates the total number of series (composed by  
 21 a number of *Abies alba* (thin black line), *Pinus leucodermis* (dashed line) and *P. nigra* (dotted line) specimens). The low-  
 22 pass filtered series with a 20 yr Gaussian smoother for both the reconstructions based on scaling and regression are also  
 23 depicted (5B). The reconstructions were truncated when there was fewer than 5 trees, and the gray areas in the graphs  
 24 depict the periods where the reconstruction is based on less than 10 trees (prior to 1713 CE). A comparison of the  
 25 reconstructed late summer temperature (this paper) with the one of Trouet (2014) using z-scores series, filtered with a 20 yr  
 26 Gaussian smoother (5C).

13



3  
4



5  
6

1 **Figure 6:** Spatial correlation pattern of the reconstructed late summer temperature (using the MXD chronology from the  
2 Italian Peninsula) versus the 0.5° grid CRU TS/E-OBS 13.1 August-September mean temperature, over the period of 1901-  
16 1980; correlation coefficient values of  $r > 0.29$  are statistically significant ( $p < 0.01$ ).